

E2F1 identified by promoter and biochemical analysis as a central target of glioblastoma cell-cycle arrest in response to ras inhibition

Roy Blum¹, Itay Nakdimon¹, Liat Goldberg¹, Ran Elkon², Ron Shamir³, Gideon Rechavi^{1,4} and Yoel Kloog^{1*}

¹Department of Neurobiochemistry, The George S. Wise Faculty of Life Sciences, Tel-Aviv University, Tel-Aviv, Israel

²The David and Inez Myers Laboratory for Genetic Research, Department of Human Genetics, Sackler School of Medicine, Tel-Aviv University, Tel-Aviv, Israel

³School of Computer Science, Tel-Aviv University, Tel-Aviv, Israel

⁴Department of Pediatric Hematology-Oncology, Safra Children's Hospital, Sheba Medical Center, Tel Hashomer and Sackler School of Medicine, Tel-Aviv University, Tel-Aviv, Israel

Active Ras contributes to the malignant phenotype of glioblastoma multiforme. Recent studies showed that the Ras inhibitor farnesyl thiosalicylic acid downregulates the transcription factor hypoxia-inducible factor-1 α , causing shutdown of glycolysis in U87 glioblastoma cells. Farnesyl thiosalicylic acid also inhibited the growth of U87 cells. The way in which Ras inhibition affects U87 cell proliferation was not clear. Here we applied a computational method in which gene expression profile clustering is combined with promoter sequence analysis to obtain global dissection of the transcriptional response to farnesyl thiosalicylic acid in U87 cells. The analysis revealed a prominent Ras-dependent cell-cycle arrest response, in which a major component is highly enriched for the binding-site signature of the transcription factor E2F1. Electrophoretic mobility shift assays together with E2F-luciferase reporter assays showed that E2F1 was inactivated by the Ras inhibitor. Inhibition of Ras by farnesyl thiosalicylic acid promoted proteasomal degradation of cyclin D1, with a concomitant decrease in phosphorylated retinoblastoma protein accompanied by downregulation of E2F1 and decreased expression of key E2F1-regulated genes critical for cell-cycle progression. U87 cell growth arrest induced by farnesyl thiosalicylic acid was overridden by constitutive expression of E2F1. Thus, downregulation of E2F1 and of hypoxia-inducible factor-1 α represents 2 distinct arms of the antioncogenic effect of Ras inhibitors in glioblastoma.

© 2006 Wiley-Liss, Inc.

Key words: ras; glioblastoma; ras inhibitors; FTS; E2F1

Overexpression and activation of receptor tyrosine kinases (RTKs) lead to proliferation of malignant astrocytoma and glioblastoma multiforme (GBM), the most frequent types of primary human brain tumors.¹ The activated RTKs trigger several common pathways, in particular those leading to activation of Akt and Ras proteins.¹ The active GTP-bound Ras proteins, through their downstream effectors, including Raf, phosphatidylinositol-3-OH kinase (PI3-K) and Ral-guanine nucleotide exchange factors, promote cell-cycle progression, cell survival and cell migration.^{2,3} Although activating (oncogenic) mutations, commonly found in many human tumors,⁴ are not prevalent in human gliomas, the abundant presence of Ras-GTP in these tumors⁵ and in glioblastoma cell lines⁶ is well documented. The increased presence of Ras-GTP in glioblastoma appears to be secondary to mitogenic signals originating from activated RTKs.¹ It follows that receptor-mediated activation of Ras signaling might be required for the progression of the glioma cell cycle. Consistent with this suggestion are the findings that the pharmacological inhibition of Ras^{6,7} or expression of dominant negative Ras in glioma cell lines⁵ result in inhibition of Ras signaling to Raf/MEK/extracellular-signal-regulated kinase (ERK) and to phosphatidylinositol-3-OH kinase (PI3-K)/Akt, with consequent attenuation of cell growth.

Recently we showed that the low-molecular-weight Ras inhibitor farnesylthiosalicylic acid (FTS) exhibits profound antioncogenic effects in U87 GBM cells. FTS inhibited active Ras and attenuated Ras signaling to extracellular ERK, PI3-K and Akt, resulting in arrest of U87 cell growth.⁶ We further showed that FTS induces disappearance of hypoxia-inducible factor (HIF-1 α), leading to down-regulated expression of key enzymes of the glycolysis pathway.⁶

Moreover, gene-expression profiling revealed that FTS alters the expression of a large group of genes that participate in cell-cycle control. Indeed, except for a metabolic group of genes, the cell-cycle genes constituted the second largest functional group whose expression was altered by FTS treatment. These observations are consistent with the possibility that the Ras inhibitor affects the prominent pathways regulating mitosis and cell-cycle progression. This possibility is strengthened by ample evidence that Ras positively regulates cyclin D1 at the transcriptional^{8–12} and translational levels¹³ and at the level of cyclin D1 protein stability, and also controls the assembly of the cyclin D1/CDK4 complex.^{14,15} Cyclin D1/CDK4 in turn phosphorylates the retinoblastoma (RB) protein,^{16–18} leading to disassembly of the RB-E2F1 transcriptional repressor complex and activation of E2F1-regulated transcription, which is critical for G1–S transition.^{16–18}

We therefore sought to identify significant transcription factors (TFs) that would participate in the FTS-induced changes in cell-cycle-associated gene profiles. We did this by using an advanced computational approach that combines clustering of the gene expression profile with the analyses of promoter sequences.

Material and methods

Analysis of gene expression data

Gene expression profiling of untreated U87 cells (0 time and 24-h and 48-h vehicle controls) and of cells treated with 70 μ mol/l FTS for 24 or 48 h (a single microarray for each condition) was performed earlier using Affymetrix Human Genome Focus oligonucleotide arrays, and a list of 5054 ‘‘valid genes’’ obtained by the microarray analysis was presented.⁶ Prior to clustering, the expression levels of each gene were standardized as ‘‘mean’’ equal to zero and ‘‘variance’’ equal to one. The EXPANDER program¹⁹ was used to discover and analyze prominent expression patterns. EXPANDER includes the CLICK algorithm for clustering of expression patterns²⁰ and the PRIMA algorithm²¹ for detecting TF binding-site signals that are enriched in the promoters of a cluster of genes. When provided with target sets and a background set of promoters, PRIMA performs statistical tests to identify TFs, whose binding-site signatures are significantly overrepresented in any of the target sets relative to the background set (TF enrichment is indicated by *p*-value). For analysis, each gene cluster was considered a

Abbreviations: Ab, antibody; EMSA, electrophoretic mobility shift assay; ERK, extracellular signal-regulated kinase; FTS, farnesylthiosalicylic acid; GBM, glioblastoma multiforme; GFP, green fluorescent protein; GSK3 β , glycogen synthase-3 β ; HIF-1 α , hypoxia-inducible factor 1 α ; PI3-K, phosphatidylinositol-3-OH kinase; RB, retinoblastoma; RTK, receptor tyrosine kinase; TF, transcription factor.

Grant sponsors: The Jacqueline Seroussi Memorial Foundations for Cancer Research; The Wolfson Foundation.

*Correspondence to: Department of Neurobiochemistry, The George S. Wise Faculty of Life Sciences, Tel-Aviv University, 69978 Tel-Aviv, Israel. Fax: 972-3-6407643. E-mail: kloog@post.tau.ac.il

Received 14 May 2005; Accepted 8 November 2005

DOI 10.1002/ijc.21735

Published online 22 February 2006 in Wiley InterScience (www.interscience.wiley.com).

target set, while the list of "valid genes" was used as the background set. PRIMA default parameters were used.²¹ Functional analysis was performed with the EASE software,²² which calculates enrichment of GO (Gene Ontology) functional categories in the target set when compared with the background set (functional category enrichment is represented by an EASE score). The group of genes of interest was used as a target set, while the list of "valid genes" was used as the background set.

Cell culture and reagents

The glioblastoma cell lines used and their growth conditions (U87, LN229, DBTRG-05MG (20/20) and U373) have been described previously.⁶ U87 cells stably expressing E2F1 (U87-E2F1 cells) were established by transfection with pcDNA3-E2F1 expression vector followed by G418 (1 mg/ml) selection. FTS was prepared as described.²³ Cells were plated at density of 2.5×10^5 cells in 6-well plates for immunocytochemical assays and for assays of luciferase reporter gene, and at a density of 1.5×10^6 cells in 10-cm dishes for all other assays. Twenty-four hours after plating we added drugs or vehicle (0.1% DMSO) to the cells. FTS was added at the concentrations indicated, U0126 at 30 $\mu\text{mol/l}$ and LY294002 at 40 $\mu\text{mol/l}$. Hoechst dye 33258 was from Sigma-Aldrich (St. Louis, MO); the enhanced chemiluminescence (ECL) kit was from Amersham (Arlington Heights, IL); mouse anti- β -tubulin Ab (AK-15) and monoclonal mouse antiphospho-retinoblastoma (pS⁷⁹⁵) Ab (R6878) were from Sigma-Aldrich; rabbit anti-cyclin D1 (M-20), rabbit anti-RB (C-15), rabbit anti-E2F1 (C-20), monoclonal mouse anti-E2F1 Ab (KH95), rabbit anti-CDC6 (H-304), rabbit anti-MCM5 (H-300) and mouse anti-c-Myc (C-33) were from Santa Cruz Biotechnology (Santa Cruz, CA); peroxidase-goat anti-mouse IgG and peroxidase-goat anti-rabbit IgG were from Jackson ImmunoResearch Laboratories (West Grove, PA); carbobenzoxy-L-leucyl-L-leucinal Z-LLL-CHO (MG132), LY294002, and U0126 were from Calbiochem (La Jolla, CA).

Cell proliferation and cell cycle assays

We plated 1.5×10^3 cells in 96-well plates for cell proliferation assays. The cells were treated 24 h after plating with different concentrations of FTS or with the vehicle (0.1% DMSO). Cell proliferation was determined after 3 days by using the [3-(4,5-dimethylthiazol-2-yl)-2,5-diphenyl]tetrazolium bromide (MTT) assay, which determines mitochondrial activity in living cells. The cells were incubated with 0.1 mg/ml MTT for 1 h at 37°C then lysed with 100% DMSO. Results were quantified by reading the optical density at 570–630 nm. For the FACS analysis we plated 1×10^6 cells in 10-cm dishes. At the next day 75 $\mu\text{mol/l}$ FTS or the vehicle 0.1% DMSO were added. After 36 h the cells were collected and suspended with PBS containing propidium iodide (50 $\mu\text{g/ml}$) (Sigma) and 0.05% Triton X-100 (BDH, Poole, UK) for nuclear staining, then analyzed with a fluorescence-activated cell sorter (FACS Caliber, Becton Dickinson).

Statistical analysis

All assays were performed in triplicate or quadruplicate. Data were expressed as mean \pm SD. Statistical significance was determined by an unpaired Student's *t*-test.

Immunoblotting assays of cell-cycle regulators

To examine the effects of FTS on cyclin D1, pRB, ppRB, E2F1, CDC6 and MCM5, we used lysates of FTS-treated or vehicle control cells and performed Western immunoblotting analysis.²⁴ Protein bands were visualized by ECL and quantified as previously described.²⁴ All biochemical and immunoblotting assays were repeated at least 3 times. Data are presented as mean \pm SD. For immunoprecipitation, lysates containing 1 mg of protein were pre-cleared with 3 μg of naive mouse IgG and protein G-Sepharose beads and then were incubated with 3 μg of mouse anti-E2F1 Ab at 4°C overnight. Immunocomplexes were incubated with protein G-Sepharose beads in excess, and the mixture was rocked at 4°C

for another 6 h. Immunoprecipitants were washed 3 times with ice-cold lysis buffer. The pellet was resuspended in $1 \times$ SDS loading buffer, boiled for 10 min, and centrifuged at 14,000 rpm for 2 min. The supernatant was collected, subjected to SDS-PAGE and Western immunoblotting with either rabbit anti-RB Ab or mouse anti-E2F1 Ab.

Immunocytochemical assays

U87 glioblastoma cells were cultured on glass coverslips and incubated with FTS, or with U0126, or with LY294002 or with vehicle, as described earlier. Alternatively, the cells were transfected with vectors (total amount of 2.3 μg DNA) encoding green fluorescent protein (GFP), GFP-H-Ras(V12), H-Ras(17N) or pcDNA3,²⁴ using the JetPEI reagent according to the manufacturer's instructions (Talron, Rehovot, Israel). Forty-eight hours after drug treatment or transfection, the cells were fixed, permeabilized, and labeled with anti-E2F1 Ab (5 $\mu\text{g/ml}$) and Cy3-conjugated donkey anti-rabbit secondary Ab (2 $\mu\text{g/ml}$), as described elsewhere.¹⁸ The cells were also labeled with Hoechst dye 33258. Typical fluorescence images of E2F1 (Cy3, red), cell nuclei (Hoechst, blue), and GFP or GFP-H-Ras(12V) (green) were collected using a fluorescence microscope (IX70, Olympus America, Melville, NY) as previously described.⁶

Plasmids

The expression vectors pEGFP-C3-H-Ras(G12V) and pRSV-H-Ras(17N) have been described previously.²⁴ pcDNA3-E2F1, E2F-luciferase reporter plasmid, pCMV-RB plasmid, and pRL-CMV plasmid²⁵ were a gift from A. Toren (Sheba Medical Center, Tel Hashomer, Israel).

Luciferase reporter gene assay

Cells were cotransfected with E2F-luc reporter plasmid (1.5 μg DNA) and pRL-CMV plasmid (0.1 μg , Renilla luciferase control reporter; Promega, Madison, WI) using 3 μl of FuGENE (Boehringer Mannheim, Mannheim, Germany). Twenty-four hours after transfection the cells were treated with FTS at the indicated concentration or with the vehicle, and then assayed for luciferase using the dual-luciferase reporter assay system (Promega, Madison, WI). The effect of RB or of dominant negative Ras on E2F activity was determined by the same procedure as that described earlier, except that the cells were not treated with drugs but were transfected with pCMV-RB (1 μg DNA) or pRSV-H-Ras(17N) (1 μg DNA). All assays were performed in triplicate and the data are presented as mean \pm SD.

Nuclear extracts and electrophoretic mobility shift assays (EMSA)

U87 cells were grown and treated with FTS as described earlier. Cells were scraped, centrifuged for 5 min at 1,000g and washed with ice-cold phosphate-buffer saline, then centrifuged again for 15 sec at 10,000g. The pellet was homogenized in ice-cold buffer A (10 mM HEPES (pH 7.4), 10 mM KCl, 0.1 mM EDTA, 0.1 mM EGTA, 1mM dithiothreitol, 0.5 mM PMSF, protease inhibitor mixture (Roche Molecular Biochemicals, Mannheim, Germany), 0.2 mM Na₃VO₄, and 0.625% NP40). The lysates were allowed to incubate for 15 min on ice and were then centrifuged for 30 sec at 10,000g. The supernatants (cytoplasmic extracts) were removed, and the nuclear pellets were resuspended in buffer C (20 mM HEPES, 0.5 M NaCl, 1 mM EDTA, 1 mM EGTA, 1 mM dithiothreitol, 0.5 mM PMSF, 0.2 mM Na₃VO₄), then vortexed for 15 min at 4°C and centrifuged for 10 min at 10,000g. The supernatants (nuclear extract) were collected and used for electrophoretic mobility shift assays (EMSA). The binding-reaction mixture, containing 10 mM Tris-HCl (pH 7.9), 60 mM KCl, 0.4 mM dithiothreitol, 10% glycerol, 2 μg bovine serum albumin, 1 μg poly(dI-dC), and 15,000 cpm of ³²P-labeled E2F1 oligonucleotides (5'-ATTTAAGTTTCGCGCCCTTTCTCAA-3') (Santa Cruz Biotechnology, CA), was incubated for 30 min with 6 μg of nuclear

extract. For specificity control, a 100-fold excess of unlabeled consensus oligonucleotides was incubated for 30 min at room temperature with radiolabeled probe. Supershift EMSA was performed by preincubating the nuclear extracts, as described earlier, with 0.5 μ g anti-E2F1 rabbit polyclonal antibodies or 0.5 μ g anti-c-Myc mouse polyclonal antibodies (as control) for 1 h at room temperature. Products were analyzed on 5% acrylamide gels made up in 1 \times TGE (50 mM Tris, 400 mM glycine, 2 mM EDTA). Dried gels were exposed to Kodak BioMax X-ray film (Kodak, Rochester, NY). Quantitative data were obtained by phosphorimaging analysis (Molecular Dynamics, Sunnyvale, CA).

Real-time PCR analysis

Extracts of total RNA (1 μ g) from cells treated with FTS (70 μ mol/l) or vehicle (control) for 48 h were reverse-transcribed in a total volume of 20 ml using the iSCRIPT cDNA Kit (Bio-Rad Laboratories, Hercules, CA). The cDNA samples were then used for real-time PCR (Syber Green PCR Kit, Roche Diagnostics, Mannheim, Germany). For the *CDC2* gene we used the forward 5'-ACT-GGC-TGA-TTT-TGG-CCT-TG-3' primer and the reverse 5'-TTG-AGT-AAC-GAG-CTG-ACC-CCA-3' primer; for the *CDC6* gene we used the forward 5'-AGG-AAA-CGT-CTG-GGC-GAT-G-3' primer and the reverse 5'-TCT-TGC-CTT-GCT-TTG-GTG-G-3' primer; for the *POLA2* gene we used the forward 5'-GGA-GTG-ATC-TTC-GGC-TTG-AC-3' primer and the reverse 5'-TGT-GCT-TGA-GTA-TTC-GGC-TG-3' primer; for the *MCM3* gene we used the forward 5'-GCA-GAC-TCA-CAG-GAG-ACC-AAG-3' primer and the reverse 5'-ATG-AGC-TTC-CCG-GAA-CAC-ATC-3' primer; for the *MCM5* gene we used the forward 5'-ATC-TTG-TCG-CGC-TTC-GAC-A-3' primer and the reverse 5'-CGT-GCA-GAG-TGA-TGA-CAT-GCT-3' primer; for the housekeeping gene *HMBS* we used the forward 5'-TGC-ACG-ATC-CCG-AGA-C-3' primer and the reverse 5'-CGT-GGA-ATG-TTA-CGA-GC-3' primer and for the housekeeping gene *ARF1* we used the forward 5'-GAC-CAC-GAT-CCT-CTA-CAA-GC-3' primer and the reverse 5'-TCC-CAC-ACA-GTG-AAG-CTG-ATG-3' primer. PCR amplifications were carried out using the Syber Green method with the 7300 PCR System (Applied Biosystem, Foster City, CA), according to the manufacturer's instructions. cDNA samples of control and FTS-treated cells (at least 2 dilutions for each) and cDNA standards were coamplified in the same reaction plate. The standard curve demonstrated a linear relationship between the cycle threshold (Ct) values and the cDNA concentration. The relative expression of each gene was normalized using the expression levels of the housekeeping genes *HMBS* and *ARF1* as standard.

Results

Identification of major gene expression patterns in FTS-treated U87 glioblastoma cells

Ras-regulated cell growth is mediated by signaling cascades that control the transcription of genes required for cell cycle progression. A previous study by our group showed that the Ras inhibitor FTS (70 μ mol/l) induces growth arrest in U87 cells, and that this was accompanied by marked changes in gene expression as evident from DNA microarray analysis of cell samples tested at 0 time and after 24 h and 48 h of drug treatment or of vehicle-treated controls.⁶ Of 5,054 "valid genes" examined in that study, 1,212 were "active genes" at least at one time point.⁶ To discover prominent expression patterns in the microarray data, in the present study, we searched for active genes whose expression was altered by at least 2-fold relative to the matching vehicle control. Our search yielded a group of 376 genes, which we then subjected to cluster analysis by CLICK, a clustering algorithm that balances intracluster homogeneity and intercluster separation.²⁰ Prior to clustering, the expression levels of each gene were standardized so that the mean was equal to zero and the variance equal to 1.0, as previously described²⁰; hence, genes clustered together share expression patterns across the tested conditions, but might differ

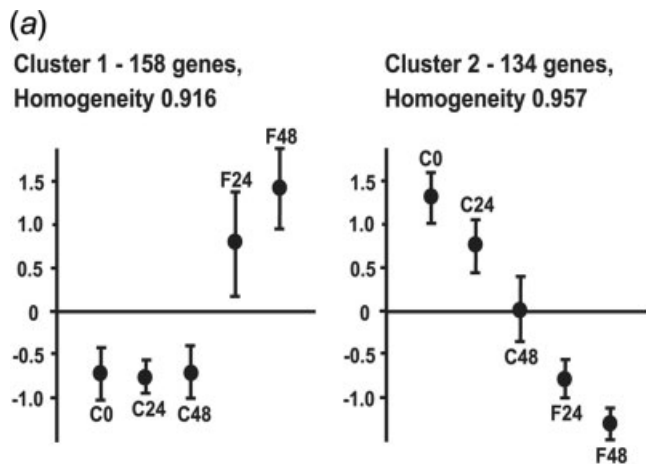
in the magnitude of their expression. In the group of 376 genes, CLICK identified 2 major clusters with high homogeneity (homogeneity values ranging between -1 and +1, where the latter represents perfect correlation between all genes in the cluster). Cluster 1, with very high homogeneity (0.916), contained 158 genes whose expression was increased by the FTS treatment (Fig. 1a). Cluster 2, with even higher homogeneity (0.957), contained 134 genes whose expression was decreased by the FTS treatment (Fig. 1a). A third, smaller cluster, consisted of 84 genes whose expression was decreased by FTS treatment, exhibited a more complex pattern and was significantly less homogeneous (0.815) than the other 2 clusters (not shown). The significantly high homogeneity of the first 2 clusters would suggest that the coclustered genes in each of these clusters are regulated by common TFs that were affected by the Ras inhibitor.

On the assumption that genes that exhibit similar transcriptional expression patterns across multiple conditions share *cis*-regulatory elements in their promoters, we performed promoter analysis using EXPANDER,²¹ a computational tool that seeks out common sequence elements (i.e., sequences that serve as binding sites for TFs). In cluster 3, EXPANDER did not detect any TF with a binding site profile that was overrepresented. As shown in Figure 1b, in cluster 1 EXPANDER identified a single overrepresented transcription factor-binding site signature (TATA), with a *p*-value of 8.77×10^{-5} (where *p* represents the statistical significance of enrichment of the TF signature in the cluster relative to the background of "valid genes"). In cluster 2 EXPANDER identified 3 TFs, namely E2F4/DP1, NF-Y, and E2F1, with *p*-values of 5.2×10^{-9} , 3.22×10^{-6} , and 1.62×10^{-9} , respectively. These results are in line with the previously described regulation of E2F1²⁶ and of NF-Y²⁷ by Ras. It is important to note that the Ras/E2F1 signaling pathway plays a key role in the mitotic processes of glioblastoma.²⁸ Increased E2F1 activity and high levels of active Ras are typically found in most GBMs.²⁸ EXPANDER identified 25 promoters that contained at least 1 high-scoring putative E2F1-binding site (Table 1). Indeed, several of these genes (including *ASK*, *CDC6*, *DNMT1*, *MCM2*, *MCM3*, *MCM5*, *MCM6*, *MSH2*, *PCNA*, *POLE*, *POLE2*, *TYMS*) are reportedly under direct control of E2F1, while the others might represent novel putative E2F1 targets.²⁹

Clearly, then, the results of the EXPANDER promoter analysis point to a major effect of the Ras inhibitor on E2F1 and consequently on genes regulated by this important TF. We therefore examined the functional relevance of these genes. Functional analysis of the 25 E2F1-regulated genes, using the EASE software tool,²² showed extremely high enrichment in those related to S-phase, DNA replication, and DNA replication-initiation categories (see Tables 1 and 2). Interestingly, similar analysis of the non-E2F1 genes in cluster 2 showed enrichment of these genes in other categories, namely those related to mitotic cell cycle, M phase and cell proliferation. The observed difference in gene enrichment between the categories reemphasizes the power of EXPANDER to assign a known biological function to its specific TF. This finding is supported by a previous demonstration that E2F1 regulates genes involved in the S-phase of the cell cycle.²⁹ Altogether our analysis indicates that a clear FTS-related gene-expression signature is associated with the inhibition of E2F1-regulated genes in U87 cells.

FTS decreases the expression of genes regulated by E2F1

Next we carried out a real-time PCR analysis to validate the gene-expression profiling and verify the results of the EXPANDER analysis. The analysis showed that FTS reduces the expression (values [mean \pm SD] represent the fold decrease in expression relative to control) of *MCM3* (2.63 ± 0.03) and *MCM5* (6.66 ± 0.01), key components of the prereplication complex involved in the formation of replication forks and in the recruitment of other DNA replication-related proteins; *CDC2* (33.33 ± 0.003) and *CDC6* (11.11 ± 0.01), regulatory cyclins important for cell cycle control; and *POLA2* (4.54 ± 0.04), a central participant in DNA replication. The decrease in the expression of genes of the



(b)

Transcription factor	Cluster number	Accession number in TRANSFAC database	Relative frequency	<i>p</i> -value
TATA	1	M00252	2.25	8.77×10^{-5}
E2F1	2	M00940	3.461	1.62×10^{-9}
E2F4/DP1	2	M00738	4.674	5.2×10^{-9}
NF-Y	2	M00287	1.712	3.22×10^{-6}

FIGURE 1 – E2F1 is the major TF affected by FTS in U87 cells. (a) Cluster analysis by EXPANDER identified 2 major clusters with very high homogeneity values. Cluster 1 contained 158 genes whose expression was increased by the FTS treatment, and cluster 2 contained 134 genes whose expression was decreased by the FTS treatment. The *x*-axis corresponds to the following conditions: samples of cells at the zero time point (C0), and after treatment for 24 h (C24) or 48 h (C48) with vehicle or FTS (F24 and F48). The *y*-axis represents the averages of standardized gene expression values. Error bars display the measured standard deviation. The total number of genes in each cluster and the cluster homogeneity value are indicated. (b) TFs whose binding site profiles were enriched in the 2 clusters. EXPANDER identified significant enrichment for 3 TFs in cluster 2, as indicated by the *p*-values shown; the most significant factor was E2F1. The *p*-values indicate the statistical significance of enrichment of the TF signature in the cluster relative to the background of “valid genes”. Relative frequency values indicate the frequency of the TF signature in a cluster divided by its frequency in the background set.

TABLE I – SUMMARY OF 25 E2F1-REGULATED GENES WHOSE EXPRESSION WAS DECREASED BY FTS TREATMENT

Affymetrix ID	Gene	Title	Fold
204244_s_at	<i>ASK</i>	Activator of S phase kinase	3
205345_at	<i>BARD1</i>	BRCA1 associated RING domain 1	24.3
222201_s_at	<i>CASP8AP2</i>	CASP8 associated protein 2	2.6
204826_at	<i>CCNF</i>	Cyclin F	2.1
203968_s_at	<i>CDC6</i>	CDC6 cell division cycle 6 homolog	3.5
204510_at	<i>CDC7L1</i>	CDC7 cell division cycle 7-like 1	2.8
201697_s_at	<i>DNMT1</i>	DNA (cytosine-5-)-methyltransferase 1	3
218530_at	<i>FHOD1</i>	Formin homology 2 domain containing 1	7.5
221521_s_at	<i>L0C51659</i>	HSPCO37 protein	42.2
202107_s_at	<i>MCM2</i>	MCM2 minichromosome maintenance deficient 2	2.6
201555_at	<i>MCM3</i>	MCM3 minichromosome maintenance deficient 3	4.3
216237_s_at	<i>MCM5</i>	MCM5 minichromosome maintenance deficient 5	9.2
201930_at	<i>MCM6</i>	MCM6 minichromosome maintenance deficient 6	4.9
209421_at	<i>MSH2</i>	mutS homolog 2, colon cancer, nonpolyposis type 1	2
202911_at	<i>MSH6</i>	mutS homolog 6	3
201202_at	<i>PCNA</i>	Proliferating cell nuclear antigen	4.3
213226_at	<i>PMSCL1</i>	Polymyositis/scleroderma autoantigen 1	9.2
216026_s_at	<i>POLE</i>	Polymerase (DNA directed), epsilon	8
205909_at	<i>POLE2</i>	Polymerase (DNA directed), epsilon 2 (p59 subunit)	3
205296_at	<i>RBL1</i>	Retinoblastoma-like protein 1	3.2
204127_at	<i>RFC3</i>	Replication factor C (activator 1) 3	7.5
205339_at	<i>SIL</i>	TAL1 (SCL) interrupting locus	13.9
201589_at	<i>SMC1L1</i>	SMC1 structural maintenance	3.5
204822_at	<i>TTK</i>	TTK protein kinase	59.7
202589_at	<i>TYMS</i>	Thymidylate synthetase	11.3

cell-cycle pathway was also manifested at the protein level. This is shown by the observed decrease in the amounts of 2 important key enzymes, MCM5 and CDC6 (Fig. 2).

FTS inhibits E2F1 DNA-binding activity

Because the results of our promoter analysis suggested that E2F1 is significantly inactivated by treatment with FTS, we next

examined whether FTS treatment was followed by a change in DNA-site occupancy of the E2F1 promoter. We did this by using the electrophoretic mobility shift assay (EMSA) of U87 cells incubated for 48 h with various concentrations of FTS. Extracts of nuclear protein from the cells were then incubated with radioactively labeled double-strand consensus oligonucleotides of E2F1-binding sites and analyzed for DNA-binding activity, i.e., for the ability of E2F1 found in the nuclear extracts to bind the labeled DNA probe.

TABLE II – PUTATIVE E2F1 TARGETS ARE EXTREMELY ENRICHED FOR S-PHASE AND FOR DNA REPLICATION FUNCTIONAL CATEGORIES

Functional Category	Cluster 2-EASE score	
	E2F1 genes (25 genes)	non-E2F1 genes (95 genes)
DNA replication and chromosome cycle	7.32×10^{-18}	5.73×10^{-9}
S-phase of mitotic cell cycle	5.43×10^{-17}	2.94×10^{-5}
DNA replication	5.43×10^{-17}	2.94×10^{-5}
DNA-dependent DNA replication	5.08×10^{-14}	1.08×10^{-2}
DNA metabolism	9.64×10^{-14}	7.38×10^{-4}
DNA replication initiation	5.17×10^{-8}	Not represented
Nucleus	5.7×10^{-8}	3.2×10^{-4}
Nucleobase, nucleoside, nucleotide and nucleic acid metabolism	1.44×10^{-7}	5.67×10^{-1}
M-phase	Not represented	6.05×10^{-11}
Mitosis	Not represented	2.56×10^{-12}
Spindle	Not represented	1.71×10^{-6}

The 134 genes in cluster 2 were subjected to promoter analysis and the results of the EASE functional classification of the group of E2F1-regulated genes (“E2F1 genes”) and the group of non-E2F1-regulated genes (“non-E2F1 genes”) are shown. The functional analysis showed an extremely high enrichment in the E2F1 genes related to S-phase and DNA replication. On the other hand, in the non-E2F1 genes the high enrichment was for entirely different categories that are related to mitotic cell cycle, M phase, and cell proliferation. “Not represented,” Functional category with non-represented genes.

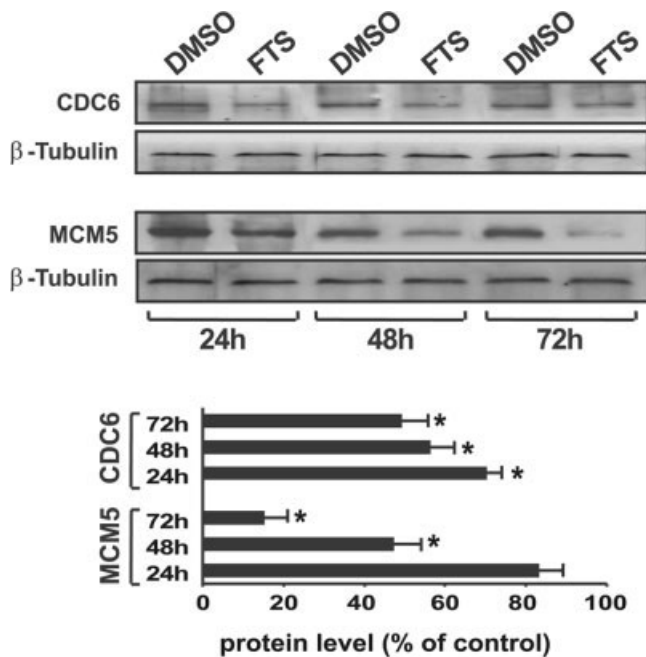


FIGURE 2 – FTS downregulates E2F1-regulated proteins in U87 GBM cells. Cells were treated with 0.1% DMSO or 75 $\mu\text{mol/l}$ FTS for the indicated times, then lysed and subjected to SDS-PAGE and immunoblotting using anti-CDC6 or anti-MCM5 Abs. Samples of total cell lysates were also immunoblotted with anti- β -tubulin Ab (loading control). Immunoblots of a typical experiment are shown. The experiment was performed 3 times and results of densitometric analysis are shown in the lower panel. Data represent mean \pm SD. * $p < 0.005$, control relative to FTS treatment.

To demonstrate the E2F1 specificity of the shifted bands, we exposed nuclear proteins isolated from control cells (DMSO-treated) to 100-fold excess of unlabeled consensus oligonucleotides and then incubated them with the radiolabeled probe (DMSO + E2F1 consensus). As shown in Figure 3a, E2F1 complex formation was abundant in the controls (DMSO), in which complex formation was specifically blocked by the excess of the unlabeled consensus oligonucleotides. Further conformation of specificity came from supershift analysis using anti-E2F1 antibody (Fig. 3b). As shown, the addition of anti-E2F1 antibodies to the nuclear extracts resulted in a supershift of the labeled probe (Fig. 3b, lane

4) while the addition of control c-Myc antibody had no effect on the mobility (Fig. 3b, lane 2).

Quantitative comparison of the E2F1-binding complexes of the control and the FTS-treated cells disclosed a clear dose-dependent decrease: treatment with FTS at a concentration of 60, 75 or 90 $\mu\text{mol/l}$ FTS caused a decrease (mean \pm SD, $n = 4$) of $41.5 \pm 1.6\%$ ($p < 0.001$), $69.6 \pm 2\%$ ($p < 0.001$), or $(75.4 \pm 1)\%$ ($p < 0.001$), respectively, in the apparent amounts of E2F1-binding complexes. This would be consistent with a decrease in the amounts of E2F1 and hence its transcriptional activity.

FTS reduces the transcriptional activity of E2F1

Next we examined whether treatment of U87 cells with FTS alters the transcriptional activity of E2F1. We used a luciferase reporter-gene assay in which luciferase expression is under the control of a minimal promoter containing 3 E2F1-binding sites in tandem.²⁵ As a control for the assay we used cells cotransfected with the reporter gene and with the RB expression vector. RB binds E2F1 and neutralizes its transcriptional activity.^{16–18} The results of these experiments (Fig. 3b) demonstrated that endogenous E2F1 is sufficient to induce significant expression of the luciferase reporter gene in U87 cells, and that expression of RB indeed causes a strong decrease ($(85.2 \pm 2.8)\%$) in reporter-gene expression. FTS treatment also induced a dose-dependent decrease in expression of the luciferase reporter gene (Fig. 3b). The decrease observed with FTS ($(83 \pm 4.3)\%$) at 90 $\mu\text{mol/l}$ was as strong as that observed with RB. The effect of FTS on expression of the luciferase reporter gene was mimicked by the expression of the dominant-negative mutant H-Ras(17N), which induced a decrease of $(63.1 \pm 4.2)\%$ (Fig. 3b). Taken together, these results strongly suggested that inhibition of Ras by FTS (or by dominant negative Ras) downregulates the transcriptional activity of E2F1 in U87 cells. This suggestion is consistent with the knowledge that E2F1 is under the positive control of Ras,²⁶ and with the previous demonstration that FTS reduces the levels of active Ras, phospho-ERK, active PI3-K and phospho-Akt in U87 cells.⁶

FTS induces proteasomal degradation of cyclin D1 and decreases retinoblastoma phosphorylation

Two distinct Ras pathways mediate the positive control of E2F1 by Ras. One is the Raf/MEK/ERK pathway, which increases cyclin D1 mRNA levels and increases cyclin D1/CDK4 assembly.^{8–12} The other is the PI3-K/Akt/GSK3 β pathway.^{14,15} GSK3 β phosphorylates cyclin D1, thereby targeting it to the ubiquitin-proteasome protein degradation pathway.^{14,15} GSK3 β itself, however, is negatively regulated by Akt, which phosphorylates and inacti-

vates it. Therefore, a Ras/PI3-K/Akt signal eliminates the GSK3 β -mediated degradation of cyclin D1.^{14,15} We examined whether FTS or inhibitors of either of the earlier mentioned 2 Ras pathways would affect the levels of cyclin D1 in U87 cells. The cells were incubated for 24 or 48 h with 75 μ mol/l FTS and lysed. The lysed cells were subjected to Western immunoblot analysis with anticyclin D1 antibody (Ab). FTS caused a reduction in cyclin D1 (mean \pm SD) of (44.3 \pm 3)% or (75 \pm 2.3)%, respectively (Fig. 4a). Similar reductions in cyclin D1 were observed in U87 cells that were treated with the MEK inhibitor U0126 (Fig. 4b) or the PI3-K inhibitor LY294002 (Fig. 4b). These results suggested that FTS-induced inhibition of both Ras pathways contributes to the

decrease in amount of cyclin D1. The FTS-induced decrease in cyclin D1 was blocked by the proteasome inhibitor MG132 (Fig. 4a), suggesting that the inhibition of the Ras/PI3-K/Akt pathway relieves the inhibition of GSK3 β by Akt.

Using Western immunoblotting, we next examined the level of the phosphorylated RB (ppRB) protein, whose initial phosphorylation is mediated by the cyclin D1/CDK4 complex.¹⁶⁻¹⁸ RB is not mutated in U87 cells³⁰ and therefore the observed decrease in cyclin D1 (Fig. 4a) was expected to reduce both cyclinD1/CDK4 activity and phosphorylated RB. Consequently, the unphosphorylated RB would retain its binding to E2F1, causing the inhibition of E2F1 transcriptional activity. To examine this possibility we treated U87 cells with FTS for 24 and 48 h and used anti-RB Ab to determine the levels of RB and ppRB. We found a significant (36.5 \pm 4)% and (55 \pm 5.2)% decrease in the ppRB band at 24 and 48 h, respectively (Fig. 4c, upper left). The total amount of RB seemed to be slightly, though nonsignificantly, reduced in some experiments. However, the ratio of ppRB to the total amount of RB was markedly and significantly lower in the FTS treated cells when compared with the controls (Fig. 4c, lower left). To strengthen these observations we repeated the experiment using 2 additional approaches. First, we used specific anti-ppRB Ab (the phospho-Ser-795Ab) and found that the FTS treatment indeed caused marked reduction in ppRB protein (Fig. 4c, upper right). Second, we examined the formation of RB-E2F1 complex in control and in FTS treated U87 cells by immunoprecipitation with anti E2F1 Ab followed by immunoblotting with anti RB Ab. We found that the levels of the RB-E2F1 complex was increased in cells treated with FTS for 36, 48 and 72 h (Fig. 4c, lower right). These results are clearly consistent with the observed FTS-induced decrease in ppRB and show that the drug treatment prevented the release of E2F1 transcription factor, which can explain the FTS-induced inhibition of E2F1 transcriptional activity (Fig. 3).

The earlier mentioned effects of FTS on the cyclin D1/RB/E2F1 pathway strongly support the notion that the inhibition of U87 cell growth by FTS is at least in part a result of reduction in cyclin D1 levels. If so then overexpression of cyclin D1 should lessen the growth inhibitory effect of FTS. We thus compared the impact of FTS on growth of U87 and U251 GBM cells that express relatively low levels of cyclin D1 with its impact on growth of 20/20 GBM cells that express relatively high levels of

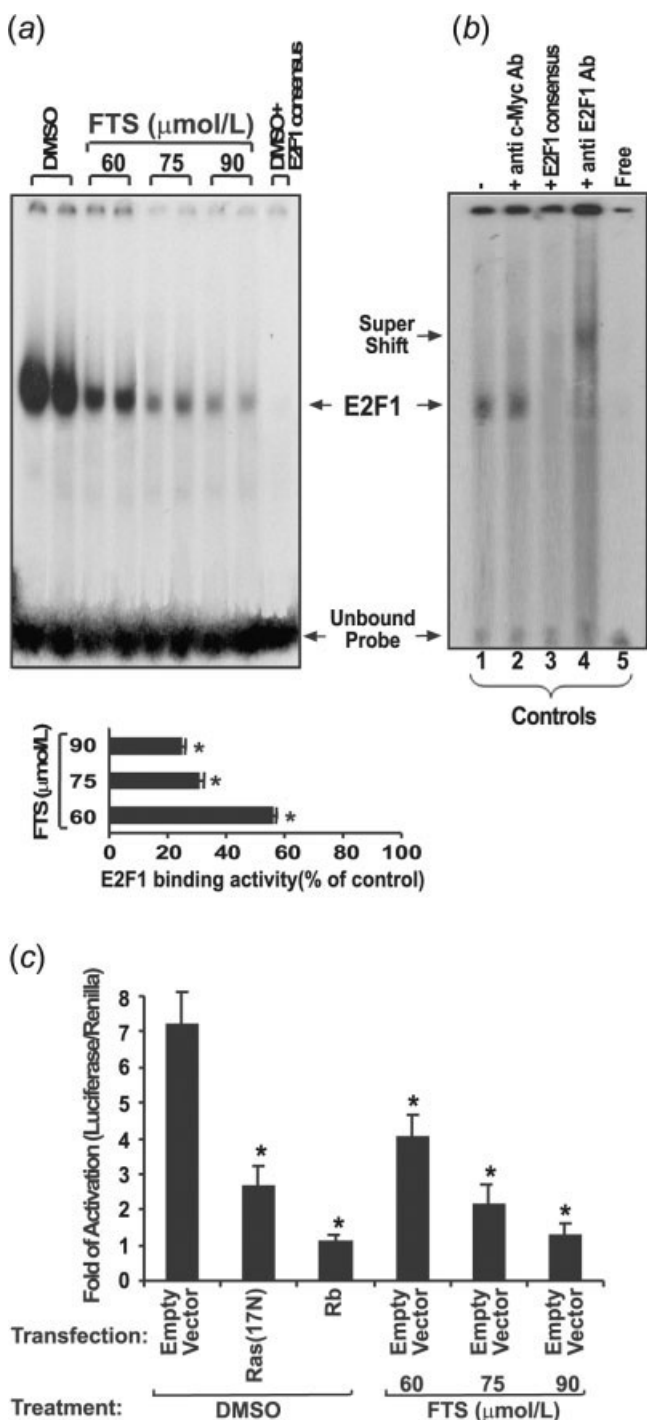


FIGURE 3 – FTS decreases DNA-binding activity and transcriptional activity of E2F1 in U87 cells. (a) FTS decreases E2F1-binding activity in a dose-dependent manner. Cells were incubated for 48 h in the absence and in the presence of the indicated concentration of FTS. Nuclear extracts were then prepared and assayed for E2F1-binding activity by EMSA, as described in Material and Methods. The arrow indicates the position of the E2F1-DNA complexes. To demonstrate the E2F1 specificity of the shifted bands, nuclear proteins isolated from control (DMSO-treated) cells were exposed to a 100-fold excess of unlabeled consensus oligonucleotides, and then incubated with radiolabeled probe (DMSO + consensus). Under these conditions the band intensity was significantly reduced. Results of a typical experiment performed in duplicate are shown. The experiment was performed twice and densitometric analysis of the results is shown in the lower panel (means \pm SD, $n = 4$); * $p < 0.001$, control relative to FTS treatment. (b) Supershift EMSA assay of the E2F1. Nuclear protein extracts from untreated U87 cells were preincubated with vehicle (lane 1), c-Myc antibody (lane 2), E2F1 consensus (lane 3) or with E2F1 antibody (lane 4) then exposed to the radiolabeled probe as described in Material and Methods. The probe without nuclear extract was loaded as a control (lane 5). (c) FTS suppresses E2F promoter activity in U87 cells. Cells were transfected with E2F-luc/pRL-CMV and then incubated for 24 h in the absence and in the presence of the indicated concentration of FTS. Alternatively, the cells were cotransfected with E2F-luc/pRL-CMV and RB or H-Ras(17N) expression vectors. The cells were then subjected to the luciferase assay as described in Material and Methods. Data represent fold activation of E2F-luciferase transcriptional activity (means \pm SD, $n = 4$); * $p < 0.05$, control relative to FTS treatment.

cyclin D1 (Fig. 4d). We found that the 20/20 cells exhibited lower sensitivity to FTS when compared with U87 and U251 cells.

FTS reduces E2F1 in GBM cell lines

Because E2F1 positively regulates its own transcription, the observed FTS-induced reduction in E2F1 transcriptional activity suggested that the inhibition of Ras by FTS or inhibition of its downstream signals by the MEK or the PI3-K inhibitor causes a decrease in E2F1 protein. We examined this possibility by 2 independent methods, Western immunoblotting and immunocytochemistry employing anti-E2F1 Ab. Immunoblot analysis was performed in FTS-treated U87 cells and in 3 additional GBM cell lines, LN229, 20/20 and U373, that express wild-type RB.³⁰ The

cells were incubated with 75 $\mu\text{mol/l}$ FTS for the indicated times, then lysed and subjected to the analysis. Results of typical experiments are shown in Fig. 5a and 5b. Treatment of U87 cells with FTS resulted in a marked decrease in E2F1 protein within 24–48 h (Fig. 5a). E2F1 was almost undetectable after 72 h of treatment, being as low as $(10 \pm 3)\%$ of the control ($p < 0.005$). Similar results were obtained with the 3 other GBM cell lines. After 48 h of FTS treatment, E2F1 was reduced to $(59.4 \pm 2.3)\%$, $(37.8 \pm 4)\%$ and $(62.3 \pm 3.7)\%$ of the control in LN229, 20/20 and U373, respectively (Fig. 5b). To examine whether the reduction in E2F1 levels was a consequence of FTS-induced growth arrest, we determined the impact of FTS in U87 cells, whose growth was arrested by serum deprivation prior to the addition of the drug. Serum deprivation that strongly inhibited U87 cell growth (not shown) was accompanied, as expected, by reduction in the amount of E2F1 (Fig. 5c). Under these conditions, where cell growth was already arrested but yet no cell death was detected, the treatment with FTS caused an almost complete disappearance of E2F1 (Fig. 5c). Thus the reduction in E2F1 seems to be a direct consequence of the inhibition of Ras pathways by FTS and not a consequence of FTS-mediated growth arrest.

For the immunocytochemical analysis, control and FTS-treated U87 cells were double-stained with rabbit anti-E2F1 Ab and then with Cy3-conjugated anti-mouse Ab (red, Cy3 fluorescence) and with Hoechst to label the cell nuclei (blue). Typical dual fluorescence images (shown in Fig. 6a) demonstrate localization of E2F1 almost exclusively to the cell nuclei of the control cells, in which FTS treatment caused a marked reduction in nuclear E2F1 (Fig. 6a). By expressing the number of cells exhibiting nuclear E2F1 as a percentage of the total number of cells, we showed that FTS caused disappearance of E2F1 from 80% of the cells (Fig. 6a). Comparable effects on nuclear E2F1 were observed in U87 cells treated with the MEK inhibitor U0126 and the PI3-K inhibitor LY294002 (Fig. 6a). Taken together, these findings supported the results obtained by Western immunoblotting and indicated that the Ras inhibitor FTS, as well as the Ras-pathway inhibitors, causes a reduction in nuclear E2F1.

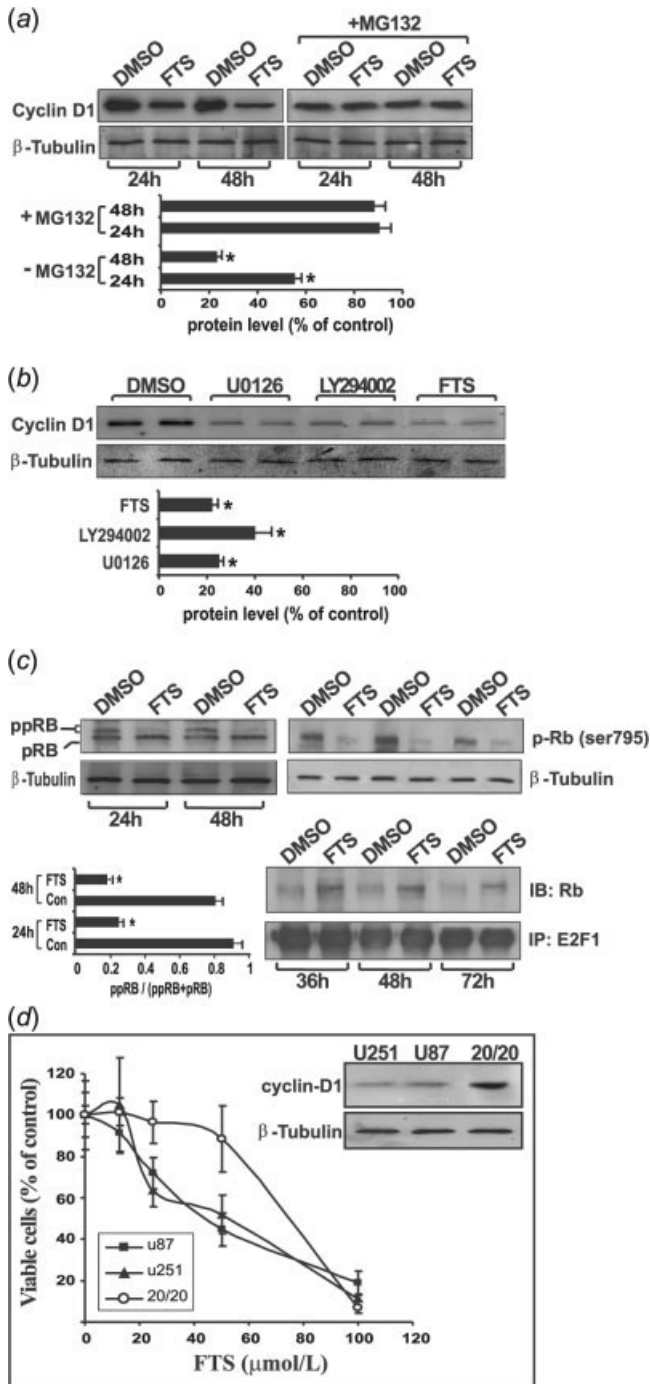


FIGURE 4 – The relationships between cyclin D1/RB phosphorylation and cell growth in FTS treated GBM cells. (a) FTS induces proteasomal degradation of cyclin D1 in U87 GBM cells. Cells were incubated for the indicated times with 0.1% DMSO or 75 $\mu\text{mol/l}$ FTS with or without 5 $\mu\text{mol/l}$ MG132 then processed for determination of cyclin D1. Results of representative experiments (each performed 3 times) are shown and densitometric analysis is given in the lower panel. (b) Effects of U0126 (30 $\mu\text{mol/l}$), LY294002 (40 $\mu\text{mol/l}$), or FTS on the levels of cyclin D1. U87 cells were treated with the inhibitors as in panel a and then processed for determination of cyclin D1. Results of representative experiments (each performed 3 times) are shown and densitometric analysis is given in the lower panel. (c) Effects of FTS on the levels of ppRB and of pRB-E2F1 complex. U87 cells were treated with FTS as in panel a and then subjected to the determination of pRB and ppRB using anti RB Ab (upper left) or to the determination of ppRB using phospho-Ser-795 Ab (upper right). Results of representative experiments (each performed 3 times) are shown. Densitometric analyses of the results indicated $(36.5 \pm 4)\%$ and $(55 \pm 5.2)\%$ decreases in the ppRB band at 24 and 48 h of the treatment. The left lower panel shows the decrease in the ratio of ppRB/(ppRB + pRB). Separate samples were also subjected to immunoprecipitation with anti-E2F1 Ab followed by immunoblotting with either anti-E2F1 Ab or with anti RB Ab (lower right). (d) Cyclin D1 levels determine the sensitivity of GBM cells to growth inhibition by FTS. U87, U251 and 20/20 cells were incubated with 0.1% DMSO or with the indicated concentrations of FTS for 5 days. The number of cells was then estimated by direct counting. Data are expressed in terms of percentage of DMSO control (means \pm SD, $n = 4$). Inset: levels of cyclin D1 in the various cell lines. In all experiments samples of total cell lysates were also immunoblotted with anti- β -tubulin Ab (loading control). * $p < 0.001$, control relative to drug treatments.

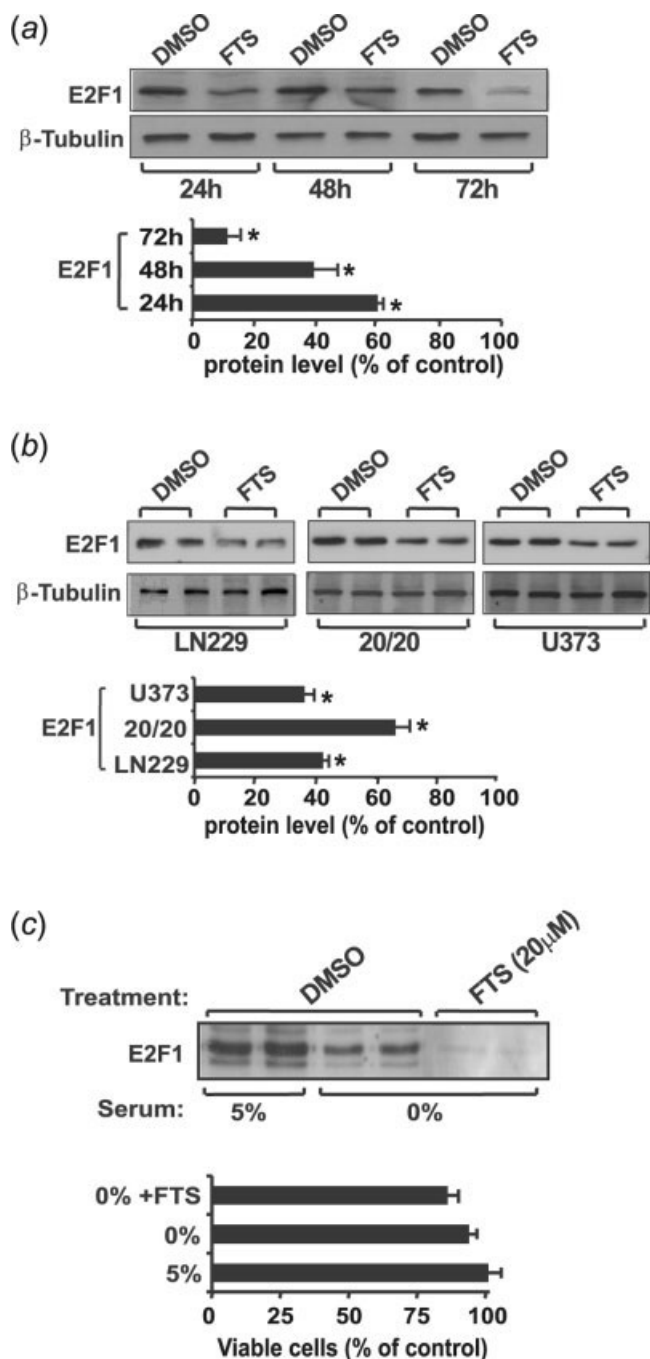


FIGURE 5 – FTS reduces E2F1 in GBM cell lines. GBM cell lines were incubated for the indicated times with 0.1% DMSO or 75 μ M/l FTS and then processed for determination of E2F1 by immunoblotting with anti E2F1 Ab. Samples of total cell lysates were also immunoblotted with anti- β -tubulin Ab. Results of representative experiments (each performed 3 times) are shown. (a) Time-dependent in E2F1 protein after treatment with FTS. (b) FTS induces a decrease in E2F1 in the GBM cell lines LN229, 20/20 and U373. The cells were grown with or without FTS for 48 h. Densitometric analyses of the results are shown in the lower panels. Data represent mean \pm SD ($n = 3$); $*p < 0.05$, control relative to drug treatments. (c) FTS reduces the levels of E2F1 in U87 cells grown in the absence of serum. The cells were first grown for 24 h in 0% serum then treated with 20 μ M/l FTS for 24 h and processed for the determination of E2F1 as in panel a. Levels of E2F1 in cells that were grown for 48 h in 5% serum are shown as well.

To further support the contention that Ras inhibition by FTS was the main cause of disruption of E2F1 nuclear accumulation, we examined the effect of dominant negative Ras on nuclear E2F1. U87 cells were cotransfected with GFP (to identify the transfected cells) and with an excess (6-fold) of the dominant-negative mutant H-Ras(17N). Controls were cotransfected with GFP and empty pcDNA3 vector. We also used cells transfected with the constitutively active GFP-H-Ras(12V) vector. The cells were then double-stained with mouse anti-E2F1 Ab, and then with Cy3-conjugated anti-mouse Ab (red, Cy3 fluorescence) and with Hoechst to label the cell nuclei (blue). Triple fluorescence images were then obtained. Typical images (Fig. 6b) demonstrate that in the control GFP-expressing cells E2F1 was localized to the cell nuclei, in which H-Ras(17N) caused a strong reduction in nuclear E2F1. In contrast, GFP-H-Ras(12V) strengthened the nuclear localization of E2F1 (Fig. 6b). By expressing the number of GFP-expressing cells exhibiting nuclear E2F1 as a percentage of the total number of cells, we showed that H-Ras(17N) caused disappearance of E2F1 from 80% of the cells whereas GFP-H-Ras(12V) caused an increase in the number of cells with nuclear E2F1 (Fig. 6b). Remarkably, the effect of H-Ras(17N) on nuclear E2F1 was indistinguishable from that of FTS.

To further evaluate the role of E2F1 deregulation by FTS in the inhibition of U87 cell growth, we established U87 cells stably expressing E2F1 (U87-E2F1 cells, Fig. 7a, left) and examined whether the forced expression of E2F1 diminishes the inhibitory effect of FTS. It is important to note that cells with highly overexpressed E2F1 undergo apoptosis³¹ and are eliminated during selection. Thus, the U87-E2F1 cell line and similarly selected clones (not shown) represent cells in which the relatively high E2F1 levels are not sufficient to induce cell death. In agreement with other earlier studies^{32,33} we found that U87-E2F1 cells grown in 5–10% serum did not exhibit an increase in S phase and enhanced growth rate. However, when such cells with forced E2F1 expression were grown in 0.5–1% serum they exhibited enhanced rate of proliferation.^{32,33} We also observed that U87-E2F1 cells grown at 1% serum, but not at high serum, exhibited an increase in growth rate when compared with U87 cells (Fig. 7a, right). U87-E2F1 cells were then treated with 75 μ M/l FTS and subjected to FACS analysis 36 h after the FTS treatment. Consistent with earlier results,⁶ we found that FTS induced a 2.5 fold decrease in S/G2 population of U87 cells (from 32.8% in control to 13.08% in the drug treated cells, Fig. 7b). Under the same conditions, U87-E2F1 cells exhibited resistance to FTS; the percentage of S/G2 population of cells was 34.88 in controls and 31.02 in the drug treated cells (Fig. 7b). Thus, constitutive expression of E2F1, unlike Ras-controlled expression of E2F1, prevents FTS from inhibiting cell cycle progression. This was further supported by results of cell proliferation assays. As shown in Figure 7c, FTS inhibited U87 cell growth in a dose dependent manner but had almost no effect on U87-E2F1 cells.

Discussion

Active Ras is abundantly present in most GBMs¹ and helps to maintain the malignant phenotype by causing transcriptional changes²⁸ that promote disruption of cell-cycle arrest and increase cell proliferation.²⁸ In a recent study by our group, in which both gene expression profiling and biochemical analyses were employed, it was shown that the Ras inhibitor FTS exhibits profound antioncogenic effects in U87 cells.⁶ Concomitantly with the inhibition of active Ras and its downstream signals, treatment with FTS also led to the disappearance of HIF-1 α and shutdown of glycolysis in U87 cells.⁶ In the present study we applied a computational method, in which clustering of gene expression profiles was combined with promoter sequence analysis to achieve global dissection of the transcriptional response to FTS in U87 cells. When focusing on the downregulated genes, EXPANDER disclosed a prominent Ras-dependent cell-cycle-arrest response with a major component that was highly enriched in binding-site profiles of the

transcription factor E2F1 (Fig. 1 and Table 2). This suggested that downregulation of this TF mediates a major aspect of the FTS-induced effects. The EMSA results, taken together with the results of E2F-luciferase reporter assays (Fig. 3), supported the contention that E2F1 is inactivated by treatment with the Ras inhibitor.

Both real-time PCR analysis and Western immunoblotting showed that FTS attenuates the expression of several key enzymes of the cell-cycle pathway that are known to be positively regulated by E2F1 (Fig. 2).

The present results are also in line with those of early experiments pointing to the significance of Ras and its pathways in cell-cycle control. Active Ras, operating via the Raf/MEK/ERK and the PI3-K/AKT/GSK3 β pathways, stimulates gene expression,⁸⁻¹² translation,¹³ and stabilization of cyclin D1.^{14,15} Cyclin D1 binds CDK4, and the active cyclinD1/CDK4 complex phosphorylates RB,¹⁶⁻¹⁸ leading to the release of E2F1 from the RB-E2F1 complex. This in turn leads to an increase in E2F1 transcriptional activity, which upregulates its own transcription and the transcription of other E2F1-regulated genes needed for S-phase progression.¹⁶⁻¹⁸ Consistent with these observations, recent studies by our group showed that the Ras inhibitor FTS attenuates Ras activation and reduces Ras signaling to ERK, PI3-K and Akt. Accordingly, inhibition of Ras by FTS promoted proteasomal degradation of cyclin D1 (Fig. 4*a,b*), with a concomitant decrease in phosphorylated RB (Fig. 4*c*). Consequently, as shown by immunoblotting (Fig. 5) and by immunocytochemistry (Fig. 6), E2F1 in FTS-treated cells was significantly downregulated. This prominent effect of FTS on E2F1 appeared to be general, as similar results were obtained with 3 other GBM cell lines (Fig. 5). Taken together these experiments provided a mechanistic explanation for the observed inhibition of U87 cell growth by FTS. In this context it is important to note that E2F1 has been reported to play a major role in human glioblastoma cell cycle progression where downregulation of E2F1 by antisense RNA resulted in a marked delay in DNA synthesis.³⁴

Although we cannot rule out the possibility that FTS affects targets other than Ras, early experiments have demonstrated significant selectivity of FTS towards active Ras. For example in Rat-1 cell the active farnesylated Ras proteins (but not the prenylated G $\beta\gamma$ -subunits of heterotrimeric G-proteins) are released from the cell membrane by FTS.³⁵ Similarly, in human melanoma cells FTS induces a decrease in the amounts of Ras but not of Rac or RhoA.³⁶ Recent experiments with K-Ras-expressing mouse glioblastoma cells have also shown that FTS induces a strong decrease in activated K-Ras but has no effect on active GTP-bound Rap, Rac or Rho proteins (Lyustikman et al., unpublished data). Finally, our experiments showed that the effects of FTS on expression of the E2F1 luciferase reporter gene and on nuclear localization of E2F1 were mimicked by expression of the dominant-negative mutant H-Ras(17N). Taken together, these results strongly suggested that it is mainly the inhibition of the Ras protein by FTS (or by dominant negative Ras) that downregulated the transcriptional activity of E2F1 in U87 cells. However, because growth

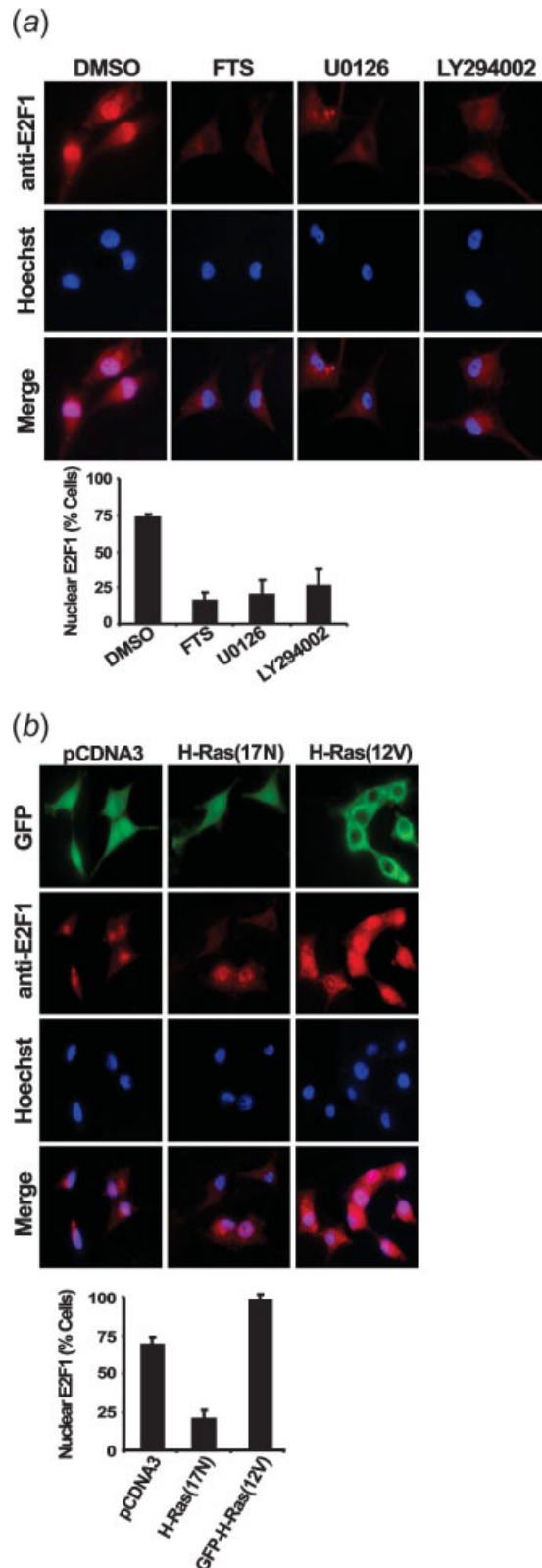


FIGURE 6 – FTS inhibits nuclear accumulation of E2F1 in U87 GBM cells. (a) U87 cells were incubated for 48 h with 0.1% DMSO or with FTS (75 μ mol/l), U0126 (30 μ mol/l) or LY294002 (40 μ mol/l). The cells were then fixed and permeabilized, labeled and visualized under a fluorescence microscope ($\times 63$ objective), as described in Material and Methods. Typical dual fluorescence images of E2F1 localization (Cy3, red) and of the cell nuclei (blue) collected in cultures under the various experimental conditions are shown along with a merged version of these images. Histogram: percentage of cells with nuclear E2F1. Bars represent the mean \pm SD of 5 samples in each case, with 100 cells per sample scored for nuclear localization of E2F1. *Significantly different from control ($p < 0.005$, Student's *t*-test). (b) U87 cells were cotransfected with 0.3 μ g GFP (to identify the transfected cells) and with 2 μ g of the dominant-negative mutant H-Ras(17N) or with 2 μ g of the constitutively active GFP-H-Ras(12V) or with 0.3 μ g GFP and 2 μ g empty pCDNA3 vector (control). The cells were then labeled and visualized as in panel a. Histogram: percentage of cells with nuclear E2F1. Bars represent the mean \pm SD of 4 samples in each case, with 100 cells per sample scored for nuclear localization of E2F1. *Significantly different from control ($p < 0.05$, Student's *t*-test).

arrest by any means would result in decreased E2F1 expression (e.g. low serum, see also Fig. 5c), we can rule out the possibility that FTS attenuated the U87 cell growth by inhibiting pathways distinct of Ras/cyclin D1-CDK4/ RB/E2F1. In this case the reduction in E2F1 levels would be a consequence of the growth arrest induced by FTS. Namely, in such a case FTS would affect additional growth-promoting pathways in U87 cells and thereby inhibited their growth. Among such pathways could be those that regulate other transcription factors such as nuclear factor- κ B,³⁷ c-Jun/

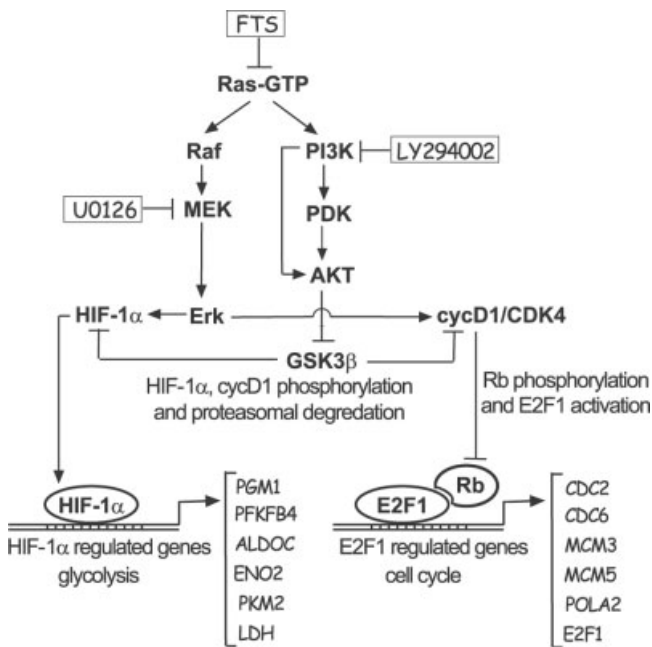
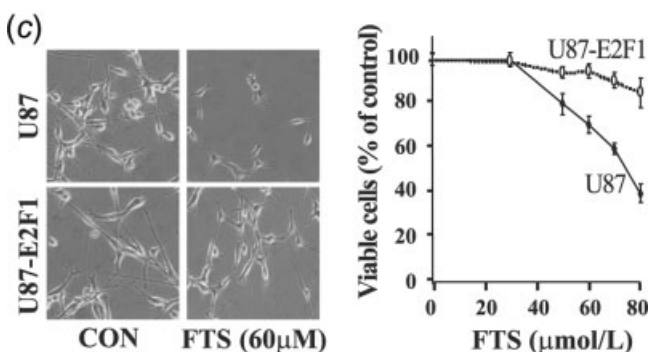
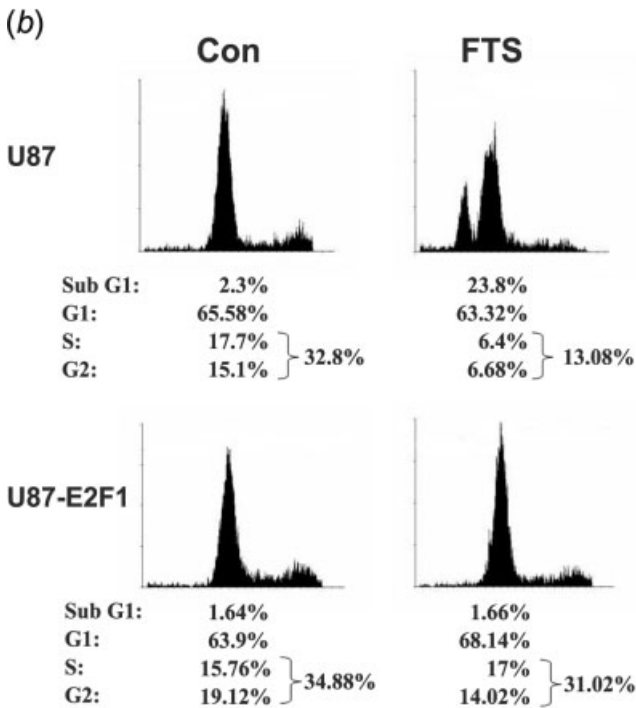
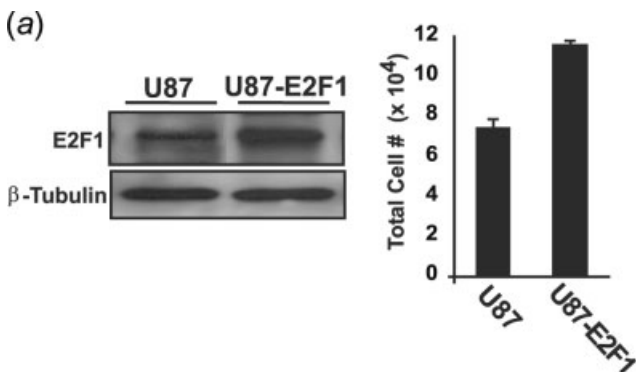


FIGURE 8 – Inhibition of Ras pathways induces cell-cycle arrest and glycolysis shut-down in GBM. Schematic representation of Ras pathways involved in regulation of cell-cycle progression and glycolysis in U87 GBM cells. Ras inhibition by FTS results in reduced ERK activation of HIF-1 α and cyclin D1/CDK4 assembly, as well as an increase in GSK3 β -mediated phosphorylation and proteasomal degradation of HIF-1 α ⁶ and cyclin D1 (present work). Inhibition of PI3-K by LY294002 or of MEK by U0126 mimics inhibition of Ras, resulting in downregulation of E2F1. Consequently, HIF-1 α and E2F1 target genes are downregulated. The scheme depicts a number of critical HIF-1 α -regulated and E2F1-regulated genes (Blum et al.,⁶ and present work) that were downregulated by FTS.

API,^{38,39} NF- κ B⁴⁰ and Myc.^{41,42} These possibilities must be investigated in future experiments.

Ample evidence attests to the strong association between the Ras/E2F1 pathway and tumorigenicity. Induction of activated Ras in HEK293 cells²⁶ and in breast adenocarcinoma cells⁴³ leads to an increase in E2F1 mRNA and protein. Ras signaling is required both for induction of cyclin D1 and for downregulation of the CDK inhibitor p27 in NIH3T3 cells.⁸ In another study it was demonstrated that transforming Ras induces transcription of cyclin D1 in human trophoblasts, mink lung epithelium, and Chinese hamster ovary fibroblast cell lines.⁹ Related studies in human gliomas showed amplification of cyclin D1,⁴⁴ CDK4,⁴⁵ or, less commonly, CDK6,⁴⁶ resulting in increased phosphorylation of RB. Also, the protooncogene MDM2, which stimulates E2F1 activity, is ampli-

FIGURE 7 – Constitutive expression of E2F1 overcomes the growth inhibitory effects of FTS. (a) U87 and U87-E2F1 cells were grown in DMEM/5% FCS then processed for determination of E2F1 by immunoblotting with anti E2F1 Ab or with anti- β -tubulin Ab (left) or grown in DMEM/1% FCS for 48 h and counted (right). Results of a representative experiment (performed 3 times) are shown. (b) FACS analysis of FTS treated U87 and U87-E2F1 cells. Cells were grown in DMEM/5% FCS and treated with 75 μ mol/l FTS for 36 h and then subjected to FACS analysis as detailed in Material and Methods. Cell cycle distribution of the control and of the FTS treated cells was monitored by flow cytometry. (c) The impact of FTS on growth of U87 and of U87-E2F1 cells. The cells were grown in DMEM/5% FCS with and without the indicated concentrations of FTS for 48 h and imaged (left). The number of viable cells was then determined by the MTT method as detailed in Material and Methods. Data are expressed as percentage of control (mean \pm SD, n = 6).

fied in a small subset of malignant gliomas.^{47,48} The ultimate target of all of the above alterations is the deregulation of E2F1, thereby fulfilling the criteria of an oncogene in GBM.²⁸ Consistent with these notions, our promoter and biochemical analysis in GBM cells spotted the Ras/E2F1 pathway as a central target that is downregulated by FTS, emphasizing the antitumorigenic effect of the Ras inhibitor.

It is important to note that in addition to the central role of Ras in cell-cycle regulation, Ras plays a critical role in regulating the control of cell survival, apoptosis, migration, metabolism and angiogenesis.⁴⁹ Many of these Ras-regulated processes involve different arms of transcriptional activities known to be deregulated in GBM. For example, GBMs depend on glycolysis, where key enzymes of the glycolytic pathway are regulated by the transcription factor HIF-1 α , which is strongly expressed in GBM.⁵⁰ A recent study by our group showed that inhibition of Ras in GBM cell lines leads to proteasomal degradation of HIF-1 α , consistent with the knowledge that Ras regulates its stability via mechanisms that involve GSK3 β -dependent and ERK-dependent phosphorylation of HIF-1 α .⁶ Gene expression profiling combined with functional clustering analysis indeed showed that inhibition of Ras in GBM induces downregulation of HIF-1 α -regulated genes, including glycolysis enzymes glucose transporter-1, VEGF-C and PDGFR.⁶ Biochemical data confirmed these observations and demonstrated that FTS induces shut-down of glycolysis in U87 cells.⁶ Nonetheless, according to our EXPANDER promoter anal-

ysis HIF-1 α was not the most overrepresented TF, whereas E2F1 was clearly overrepresented. Because EXPANDER identifies TFs whose binding-site profiles are significantly more prevalent in the target set than in the background set, these observations strongly suggested that E2F1 is a dominating TF affected by inhibition of Ras in GBM.

On the basis of our recent work⁶ and the results of the present study, we conclude that FTS suppresses 2 major pathways that are crucial for energy production and proliferation in U87 glioblastoma cells, as depicted in Figure 8. Inhibition of Ras signals to ERK and Akt downregulates HIF-1 α , leading to glycolysis shut-down,⁶ and at the same time downregulates E2F1, leading to cell-cycle arrest. The suppressive effect of FTS on cell proliferation is an indication of its potential application as a therapeutic agent for GBM.

Acknowledgements

We are grateful for the Arison family's donation to the Center of DNA Chips in Pediatric Oncology, Chaim Sheba Medical Center.

Yoel Kloog is the incumbent of The Jack H. Skirball Chair for Applied Neurobiology. Gideon Rechavi is the incumbent of the Djerassi Chair in Oncology. Ron Shamir is the incumbent of the Raymond and Beverly Sackler Chair in Bioinformatics.

We thank S.R. Smith for editorial assistance.

References

- Holland EC. Gliomagenesis: genetic alterations and mouse models. *Nat Rev Genet* 2001;2:120–9.
- Shields JM, Pruitt K, McFall A, Shaub A, Der CJ. Understanding Ras: 'it ain't over 'til it's over'. *Trends Cell Biol* 2000;10:147–54.
- Downward J. Targeting RAS signalling pathways in cancer therapy. *Nat Rev Cancer* 2003;3:11–22.
- Bos JL. Ras oncogenes in human cancer: a review. *Cancer Res* 1989;49:4682–9.
- Guha A, Feldkamp MM, Lau N, Boss G, Pawson A. Proliferation of human malignant astrocytomas is dependent on Ras activation. *Oncogene* 1997;15:2755–65.
- Blum R, Jacob-Hirsch J, Amariglio N, Rechavi G, Kloog Y. Ras inhibition in glioblastoma down-regulates hypoxia-inducible factor-1 α , causing glycolysis shutdown and cell death. *Cancer Res* 2005;65:999–1006.
- Sebt SM, Hamilton AD. Farnesyltransferase and geranylgeranyltransferase I inhibitors and cancer therapy: lessons from mechanism and bench-to-bedside translational studies. *Oncogene* 2000;19:6584–93.
- Aktas H, Cai H, Cooper GM. Ras links growth factor signaling to the cell cycle machinery via regulation of cyclin D1 and the Cdk inhibitor p27KIP1. *Mol Cell Biol* 1997;17:3850–7.
- Albanese C, Johnson J, Watanabe G, Eklund N, Vu D, Arnold A, Pestell RG. Transforming p21ras mutants and c-Ets-2 activate the cyclin D1 promoter through distinguishable regions. *J Biol Chem* 1995;270:23589–97.
- Lavoie JN, L'Allemain G, Brunet A, Muller R, Pouyssegur J. Cyclin D1 expression is regulated positively by the p42/p44MAPK and negatively by the p38/HOGMAPK pathway. *J Biol Chem* 1996;271:20608–16.
- Winston JT, Coats SR, Wang YZ, Pledger WJ. Regulation of the cell cycle machinery by oncogenic ras. *Oncogene* 1996;12:127–34.
- Weber JD, Raben DM, Phillips PJ, Baldassare JJ. Sustained activation of extracellular-signal-regulated kinase 1 (ERK1) is required for the continued expression of cyclin D1 in G1 phase. *Biochem J* 1997;326(Part 1):61–8.
- Muise-Helmericks RC, Grimes HL, Bellacosa A, Malstrom SE, Tschlis PN, Rosen N. Cyclin D expression is controlled post-transcriptionally via a phosphatidylinositol 3-kinase/Akt-dependent pathway. *J Biol Chem* 1998;273:29864–72.
- Diehl JA, Cheng M, Roussel MF, Sherr CJ. Glycogen synthase kinase-3 β regulates cyclin D1 proteolysis and subcellular localization. *Genes Dev* 1998;12:3499–511.
- Diehl JA, Zindy F, Sherr CJ. Inhibition of cyclin D1 phosphorylation on threonine-286 prevents its rapid degradation via the ubiquitin-proteasome pathway. *Genes Dev* 1997;11:957–72.
- Chen PL, Scully P, Shew JY, Wang JY, Lee WH. Phosphorylation of the retinoblastoma gene product is modulated during the cell cycle and cellular differentiation. *Cell* 1989;58:1193–8.
- DeCaprio JA, Ludlow JW, Lynch D, Furukawa Y, Griffin J, Pivnicka-Worms H, Huang CM, Livingston DM. The product of the retinoblastoma susceptibility gene has properties of a cell cycle regulatory element. *Cell* 1989;58:1085–95.
- Mihara K, Cao XR, Yen A, Chandler S, Driscoll B, Murphree AL, T'Ang A, Fung YK. Cell cycle-dependent regulation of phosphorylation of the human retinoblastoma gene product. *Science* 1989;246:1300–3.
- Sharan R, Maron-Katz A, Shamir R. CLICK and EXPANDER: a system for clustering and visualizing gene expression data. *Bioinformatics* 2003;19:1787–99.
- Sharan R, Shamir R. CLICK: a clustering algorithm with applications to gene expression analysis. *Proc Int Conf Intell Syst Mol Biol* 2000;8:307–16.
- Elkon R, Linhart C, Sharan R, Shamir R, Shiloh Y. Genome-wide in silico identification of transcriptional regulators controlling the cell cycle in human cells. *Genome Res* 2003;13:773–80.
- Hosack DA, Dennis G, Jr, Sherman BT, Lane HC, Lempicki RA. Identifying biological themes within lists of genes with EASE. *Genome Biol* 2003;4:R70.
- Marciano D, Ben Baruch G, Marom M, Egozi Y, Haklai R, Kloog Y. Farnesyl derivatives of rigid carboxylic acids-inhibitors of ras-dependent cell growth. *J Med Chem* 1995;38:1267–72.
- Elad-Sfadia G, Haklai R, Ballan E, Gabius HJ, Kloog Y. Galectin-1 augments Ras activation and diverts Ras signals to Raf-1 at the expense of phosphoinositide 3-kinase. *J Biol Chem* 2002;277:37169–75.
- Nili E, Cojocaru GS, Kalma Y, Ginsberg D, Copeland NG, Gilbert DJ, Jenkins NA, Berger R, Shaklai S, Amariglio N, Brok-Simoni F, Simon AJ, et al. Nuclear membrane protein LAP2 β mediates transcriptional repression alone and together with its binding partner GCL (germ-cell-less). *J Cell Sci* 2001;114:3297–307.
- Berkovich E, Ginsberg D. Ras induces elevation of E2F-1 mRNA levels. *J Biol Chem* 2001;276:42851–6.
- Gu Z, Kuntz-Simon G, Rommelaere J, Cornelis J. Oncogenic transformation-dependent expression of a transcription factor NF-Y subunit. *Mol Carcinog* 1999;24:294–9.
- Maher EA, Furnari FB, Bachoo RM, Rowitch DH, Louis DN, Cavenee WK, DePinho RA. Malignant glioma: genetics and biology of a grave matter. *Genes Dev* 2001;15:1311–33.
- Stevens C, La Thangue NB. E2F and cell cycle control: a double-edged sword. *Arch Biochem Biophys* 2003;412:157–69.
- Weller M, Rieger J, Grimm C, Van Meir EG, De Tribolet N, Krajewski S, Reed JC, von Deimling A, Dichgans J. Predicting chemoresistance in human malignant glioma cells: the role of molecular genetic analyses. *Int J Cancer* 1998;79:640–4.
- Mitlianga PG, Gomez-Manzano C, Kyriltis AP, Fueyo J. Overexpression of E2F-1 leads to bax-independent cell death in human glioma cells. *Int J Oncol* 2002;21:1015–20.
- Logan TJ, Jordan KL, Hall D. Altered shape and cell cycle characteristics of fibroblasts expressing the E2F1 transcription factor. *Mol Biol Cell* 1994;5:667–78.

33. Singh P, Wong SH, Hong W. Overexpression of E2F-1 in rat embryo fibroblasts leads to neoplastic transformation. *EMBO J* 1994;13:3329–38.
34. Sala A, Nicolaidis NC, Engelhard A, Bellon T, Lawe DC, Arnold A, Grana X, Giordano A, Calabretta B. Correlation between E2F-1 requirement in the S phase and E2F-1 transactivation of cell cycle-related genes in human cells. *Cancer Res* 1994;54:1402–6.
35. Haklai R, Gana-Weisz G, Elad G, Paz A, Marciano D, Egozi Y, Ben Baruch G, Kloog Y. Dislodgment and accelerated degradation of Ras. *Biochemistry* 1998;37:1306–14.
36. Jansen B, Schlagbauer-Wadl H, Kahr H, Ress E, Mayer B, Eichler HG HP, Gana-Weisz M, Ben-David E, Kloog Y, Wolff K. Novel ras antagonist blocks human melanoma growth. *Proc Natl Acad Sci U.S.A.* 1999;96:14019–24.
37. Amiri KI, Richmond A. Role of nuclear factor- κ B in melanoma. *Cancer Metastasis Rev* 2005;24:301–13.
38. Behre G, Whitmarsh AJ, Coghlan MP, Hoang T, Carpenter CL, Zhang DE, Davis RJ, Tenen DG. c-Jun is a JNK-independent coactivator of the PU. 1 transcription factor. *J Biol Chem* 1999;274:4939–46.
39. Janulis M, Silberman S, Ambegaokar A, Gutkind JS, Schultz RM. Role of mitogen-activated protein kinases and c-Jun/AP-1 transactivating activity in the regulation of protease mRNAs and the malignant phenotype in NIH 3T3 fibroblasts. *J Biol Chem* 1999;274:801–13.
40. Lee SR, Park JH, Park EK, Chung CH, Kang SS, Bang OS. Akt-induced promotion of cell-cycle progression at G2/M phase involves upregulation of NF- κ B binding activity in PC12 cells. *J Cell Physiol* 2005;205:270–7.
41. Sears R, Nuckolls F, Haura E, Taya Y, Tamai K, Nevins JR. Multiple Ras-dependent phosphorylation pathways regulate Myc protein stability. *Genes Dev* 2000;14:2501–14.
42. Sears RC, Nevins JR. Signaling networks that link cell proliferation and cell fate. *J Biol Chem* 2002;277:11617–20.
43. Fan J, Bertino JR. K-ras modulates the cell cycle via both positive and negative regulatory pathways. *Oncogene* 1997;14:2595–607.
44. Buschges R, Weber RG, Actor B, Lichter P, Collins VP, Reifenberger G. Amplification and expression of cyclin D genes (CCND1, CCND2 and CCND3) in human malignant gliomas. *Brain Pathol* 1999;9:435–42; discussion 432–3.
45. Schmidt EE, Ichimura K, Reifenberger G, Collins VP. CDKN2 (p16/MTS1) gene deletion or CDK4 amplification occurs in the majority of glioblastomas. *Cancer Res* 1994;54:6321–4.
46. Costello JF, Plass C, Arap W, Chapman VM, Held WA, Berger MS, Su Huang HJ, Cavenee WK. Cyclin-dependent kinase 6 (CDK6) amplification in human gliomas identified using two-dimensional separation of genomic DNA. *Cancer Res* 1997;57:1250–4.
47. Martin K, Trouche D, Hagemeier C, Sorensen TS, La Thangue NB, Kouzarides T. Stimulation of E2F1/DP1 transcriptional activity by MDM2 oncoprotein. *Nature* 1995;375:691–4.
48. Reifenberger G, Liu L, Ichimura K, Schmidt EE, Collins VP. Amplification and overexpression of the MDM2 gene in a subset of human malignant gliomas without p53 mutations. *Cancer Res* 1993;53:2736–9.
49. Campbell PM, Der CJ. Oncogenic Ras and its role in tumor cell invasion and metastasis. *Semin Cancer Biol* 2004;14:105–14.
50. Korkolopoulou P, Patsouris E, Konstantinidou AE, Pavlopoulos PM, Kavantzias N, Boviatis E, Thymara I, Perdiki M, Thomas-Tsagli E, Angelidakis D, Rologis D, Sakkas D. Hypoxia-inducible factor 1 α /vascular endothelial growth factor axis in astrocytomas. Associations with microvessel morphometry, proliferation and prognosis. *Neuropathol Appl Neurobiol* 2004;30:267–78.